# Dynamic electron localization initiated by particle-bath coupling

Guangqi Li, Bijan Movaghar, and Mark A. Ratner

Phys. Rev. B **87**, 094302 — Published 6 March 2013

DOI: 10.1103/PhysRevB.87.094302

# Dynamic Electron Localisation Initiated by Particle-bath Coupling

Guangqi Li,[1] Bijan Movaghar,[1] and Mark A. Ratner[1]
[1]*Department of Chemistry, Northwestern University, Evanston IL, 60208, USA*
(Dated: February 21, 2013)

We consider the quantum evolution and relaxation of an electron or hole which is coupled to a set of bath modes. In most applications the bath modes would be the vibronic coordinates but the model considered applies to any type of dynamic boson environment. The method is developed specifically for the problem of dynamic polaron formation in small non-periodic systems. It can describe a broad group of experimental situations, including in particular electron localization in organics and polymeric materials and devices. The immediate bath is allowed to dissipate energy to a secondary bath.The bath obeys classical dynamics which puts some restriction on the range of validity of this approach. Using the density matrix formalism on a tight binding model consisting of a linear chain coupled to vibronic coordinates, we demonstrate in real time how the interaction with a dissipative bath makes the initial quantum distribution reach a steady state population. This calculation is based on the Ehrenfest dynamics approximation. As an example we consider coupling at a single impurity site and find that for given parameters (bath coupling, site energy, and relaxation rate), the particle becomes dynamically localized in space on a particular time scale. This localized particle can be called a polaron. We define a population formation time in the same way as done in the experimental measurement. This formation time is studied as a function of the coupling strength, bandwidth and energy dissipation rate. Energy dissipation plays a crucial role in the spatial localization process. The formation time shortens as the electron-vibration coupling increases, and as the intersite tunneling increases, but lengthens with impurity trap depth. Polaron formation is suppressed for sufficiently wide electronic bands.

PACS numbers:

## I. INTRODUCTION

Understanding the quantum mechanical evolution and subsequent relaxation of an electron or exciton in a system with bath coupling remains a challenging problem[1–10]. The transfer of charge or energy along a molecular chain or polymeric material exemplifies the relevant systems. To make the problem straightforward and intuitive, we restrict ourselves to a linear system of sites described by the tight binding Hamiltonian. If at time t=0 we inject an electron at a given site or into a chosen electronic eigenstate in a closed electronic system with electron-vibration and vibration-phonon (environmental) coupling, the particle should eventually arrive in the ground state of the coupled system provided there are finite tunneling matrix elements to all the sites and a high enough local dissipation rate. If the coupling to the bath is very weak, this (final) state will be close to that of the uncoupled (no bath ) electronic system, because electron-vibration coupling induced shifts being considered as small. If a set of sites has in some region of the network lower energies than in the rest but the system cannot dissipate the electronic energy to build up the local populations (no electron-vibration coupling), the electron may well self-trap into a configuration where the local energy is higher compared to other sites in the network. Generally the quantum wave function will localize along the lines of Stark-Wannier[11,12] behavior when the energy differences between the sites in the downward cascade are larger than half the bandwidth. But localization could also be due to disorder (a finite-system type of Anderson localization)[13]. Switching on the electron-vibration coupling then allows the electron to relax its energy and to diffuse to arrive at the lowest level .

To ensure that the system does arrive in a given final state, introducing irreversibility via secondary bath coupling or (classically speaking) frictional dissipation and energy relaxation is essential. If the electronic tight binding chain is made very long, and the system is kept closed, it is possible for the electron-vibration coupling to lead to localized polaron formation in some parameter limits[14] even if there is no energy dissipation. Here a nearly stable final state is achieved because it is entropically unlikely that once shared to all modes, this shared energy would go back to reform the original state. But slight changes in parameters give rise to periodic breathing modes in which the polaron is periodically created and destroyed[14]. The physically realistic limit is to allow the dissipation of energy to the outside world. Therefore we will utilize the quantum relaxation methodology[15] and the closely related semi classical[16–18] one, both of which allow irreversible energy relaxation to take place. The quantum method is applied in a limit which is essentially equivalent to the semi-classical Ehrenfest method[19].

The methods developed here have a wide range of applications to problems where there is a coupling to a bosonic field which can localize or delocalize thermally charge or excitations, or to problems where this coupling induces dephasing of quantum trajectories. Topical examples are transients provided by Raman experiments[20], femto-second photo-induced absorption[9,21,22], and electron (exciton) transfer studies[23–29]; this vigorously emerging field also includes quantum and optical computing. The techniques developed here may have application in photo-induced electron transfer[30–32], and photo-generation and transfer of charge in softer materials. Femtosecond electron transfer and energy relaxation from copper into a surface layer covered with ice (image potential band) has been well studied experimentally[33].

But we should point out that the classical treatment of the bath can be a source of error. When phonon modes are slow and/or the splittings are not well resolved, the motion of ions is slow compared to the electronic degrees of freedom, the self-consistent Ehrenfest treatment is known to be a good approximation. The electrons are moving in a field of slower moving ions which depend self-consistently on the temporal distribution of the electronic charge. When phonon spectra are resolved, and splittings are comparable to or larger than the electron bandwidth, this method will tend to seriously overestimate the polaron formation times, by up to an order of magnitude[19]. The reason is that, in reality, vibrations do not only see the average evolving local charge but the actual evolving local charge. Fortunately the main discrepancy affects the formation times and not the steady state distributions. Since the full quantum solution is not tractable when more than a few vibrational modes are involved, in practical situations, it is a good starting point to use the semi-classical method, remembering where errors might occur. In the present model, the electron-phonon coupling and the impurity center are described in the Hamiltonian. The motion of the lattice is solved using a semi-classical method. Such a quasi-classical description has been used to analyze multiphonon trapping on an impurity center, in a semiconductor, and self-trapping of carriers and excitons[34,35]. This approach has also been used in the past and proved to be effective in the limit of strong electron-phonon coupling[36–38]. It was shown that in the Froehlich polaron model, the strong coupling expansion is well suited to describe the optical conductivity[34]. This is true both in the limit of the applicability of the Franck-Condon principle and beyond.

In section II we introduce the theoretical model, and in section III we apply this model to polaron formation, and discuss polaron formation for varying band coupling, electron-vibration coupling, and vibration-phonon relaxation rate. The total energy relaxation of the system is analyzed. Section IV concludes, and discusses future applications.

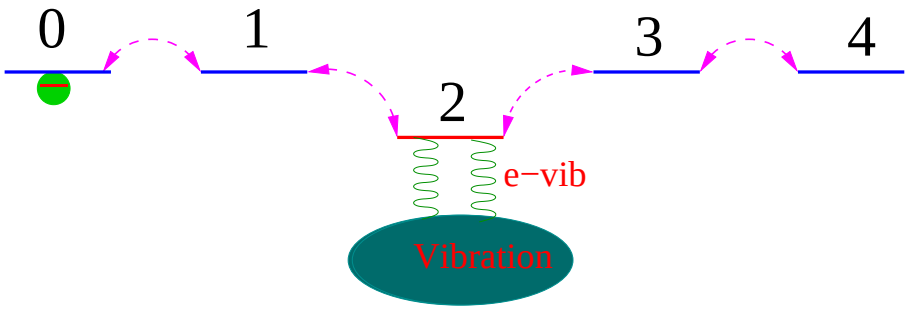


FIG. 1: The scheme of a chain including 5 sites. The electron-vibration (e-vib) interaction is added to the middle site 2.

## II. THEORETICAL MODEL

The Hamiltonian of the 5-site system in Fig. 1 is

$$H = H_S + H_B + H_{SB} \tag{1}$$

$$H_S = \sum_{l=0}^{4} \varepsilon_l c_l^\dagger c_l + \mathrm{V} \sum_{l=0}^{3} (c_l^\dagger c_{l+1} + c_{l+1}^\dagger c_l) + \hbar\omega_0 d_0^\dagger d_0 + \alpha c_2^\dagger c_2 (d_0^\dagger + d_0) \tag{2}$$

$$H_B = \sum_s \hbar\omega_s d_s^\dagger d_s \tag{3}$$

$$H_{SB} = \sum_s \beta_s (d_0^\dagger + d_0)(d_s^\dagger + d_s) \tag{4}$$

where $H_S$ is the Hamiltonian of the 5-site linear chain[54], consisting of a system of sites with orbitals coupled by the tight binding Hamiltonian with near-neighbor site coupling V and diagonal site energies $\varepsilon_l$. One site is also coupled directly to a primary vibronic mode with coordinate $d_0^\dagger + d_0$ and frequency $\omega_0$. The operators $c_l^\dagger$ ($c_l$) create (annihilate) an electron in site $l$. The last term in the right side of Eq. 2 is the electron-vibration coupling. We permit this vibronic coupling only at site 2. Besides the primary vibration, the secondary phonons (expressed in Eq. 3) with dimensionless coordinates $d_s^\dagger + d_s$ and frequencies $\omega_s$ couple to the primary vibration (Eq. 4)[55].

The electronic potential of the vibronic subspace is described in the paper[15] of Galperin, et al. as

$$H_{Ph} = \hbar\omega_0 d_0^\dagger d_0 + \alpha c_2^\dagger c_2 (d_0^\dagger + d_0) + \sum_s [\hbar\omega_s d_s^\dagger d_s + \beta_s (d_0^\dagger + d_0)(d_s^\dagger + d_s)] \ . \tag{5}$$

Further using the Langevin equation, a generalized quantum dynamics of the primary vibration is[15]

$$d_0^\dagger(t) + d_0(t) = \frac{1}{\hbar} \int_0^t d\tau D^r(t-\tau) \alpha c_2^\dagger(\tau) c_2(\tau) \ . \tag{6}$$

Here $D^r$ is the retarded green function of the active vibration.

Based on the Born-Oppenheimer approximation, we treat the bath in a classical approximation. This resembles Ehrenfest dynamics[39] and may result in substantial quantitative errors. The dimensionless displacement $q(t)$ of the primary vibration can be expressed by a time-dependent configuration as

$$q(t) =< d_0^\dagger(t) + d_0(t) >= \frac{1}{\hbar}\int_0^t d\tau D^r(t-\tau)\alpha < c_2^\dagger(\tau)c_2(\tau) > \ , \tag{7}$$

here $< d_0^\dagger(t) + d_0(t) >$ and $< c_2^\dagger(\tau)c_2(\tau) >$ indicate the average vibrational coordinate extension and the average population on site 2, respectively.

Solving the equation for the displacement $q(t)$ we note that there are two sources of displacement: i) the action of the charge itself which displaces the $q(t)$ in proportion to its population and delayed by the relaxation process and ii) the displacement caused by thermal excitations. In this paper we are concerned with zero temperature so we include only i) .

Using the wide-band approximation[15]

$$D^r(\omega) = \frac{1}{\omega + \omega_0 + i\gamma_0/2} - \frac{1}{\omega - \omega_0 + i\gamma_0/2} \tag{8}$$

and its Fourier transform

$$D^r(t) = i[e^{(i\omega_0 - \gamma_0/2)t} - e^{(-i\omega_0 - \gamma_0/2)t}] = -2sin(\omega_0 t)e^{-\gamma_0 t/2} \ , \tag{9}$$

and substituting Eq. 9 into Eq. 7, we get

$$q(t) = -\frac{2\alpha}{\hbar}\int_0^t d\tau sin[\omega_0(t-\tau)]e^{-\gamma_0(t-\tau)/2} < c_2^\dagger(\tau)c_2(\tau) > \ , \tag{10}$$

here $\gamma_0$ is the phonon relaxation rate induced by the active vibration-phonon coupling. It is obtained by taking only the imaginary part of the active phonon self energy $\Sigma$ as

$$\gamma_0(\omega)/2 = \frac{1}{\hbar}\mathrm{Im}\{\Sigma_{\mathrm{phonon}}(\omega)\} = \frac{1}{\hbar}\sum_{\mathrm{s}} |\beta_{\mathrm{s}}|^2 \delta(\hbar\omega - \hbar\omega_{\mathrm{s}}) \ . \tag{11}$$

The effective electronic system Hamiltonian can then be expressed as[15–17]

$$H_{eff} = \sum_{l=0}^{4} \varepsilon_l c_l^\dagger c_l + V\sum_{l=0}^{3}(c_l^\dagger c_{l+1} + c_{l+1}^\dagger c_l) + F(t)c_2^\dagger c_2 \ , \tag{12}$$

here $F(t)$ can be taken as the electron-vibration coupling energy and is expressed as

$$F(t) = \alpha q(t) = -\lambda_0 \int_0^t d\tau sin[\omega_0(t-\tau)] e^{-\gamma_0(t-\tau)/2} < c_2^\dagger(\tau) c_2(\tau) > \ , \tag{13}$$

with

$$\lambda_0 = 2\alpha^2/\hbar \ . \tag{14}$$

The system density matrix $\rho$ can be solved using the Liouville equation

$$i\hbar \frac{d\rho}{dt} = [H_{eff}, \rho] \tag{15}$$

with the initial condition that there is one electron at site 0.

The on-site electronic population at any time t is

$$P_l(t) =< c_l^\dagger(t) c_l(t) > \ , with \ \ \sum_{l=0}^{4} P_l(t) = 1 \ . \tag{16}$$

The total system energy is

$$E_T = E_e + E_p + E_l \tag{17}$$

with

$$E_e = \sum_{l=0}^{4} \varepsilon_l < c_l^\dagger c_l > + \mathrm{V} \sum_{l=0}^{3} < c_l^\dagger c_{l+1} + c_{l+1}^\dagger c_l > \ , \tag{18}$$

$$E_p = F(t) < c_2^\dagger c_2 > \ , \tag{19}$$

$$E_l = \frac{1}{2\lambda_0 \omega_0} \{\omega_0^2 F^2 + \dot{F}^2\} \ . \tag{20}$$

The three terms in Eq. 17 are the electron energy, the electron-vibration energy and the lattice energy respectively. Since the vibronic modes are treated classically, the lattice energy can be evaluated using the definition of the dimensionless displacement $q(t)$ in Eq. 7, to generate a mode displacement $x(t)$. So we use $E_l = \frac{1}{2} M \omega_0^2 x^2 + \frac{1}{2} M \dot{x}^2$ with $x = \frac{1}{\sqrt{2M\omega_0}} q$ to obtain Eq. 20 (details can be found in the supporting information). $M$ is the effective mass of the vibronic mode at site 2.

It is important to note that as shown in Eq. 7, and in the absence of thermal noise, the displacement coordinate "q(t)"is itself a function of the occupation of the site 2 with a time delay. This makes the

problem intrinsically non-linear and the population self-consistently controls the local displacement coordinates. If the thermal noise is included, the "q(t)"will depend both on the population and the random fluctuations induced by the environment. This approach is therefore in line with that of Lakhno[16,17] and differs from the pure fluctuation assisted transport methods used in ref[25,40,41].

It is possible to compute the trajectory of Fig.1 by i) allowing mobile electron and stationary hole to interact, ii) allowing the bath coupling to include more modes, iii) permitting the density to disappear into a sink, iv) including lattice modulation of the overlap $V[|\tilde{R}_{ij}|]$[14,42]. We here focus on describing the trajectory with a given start site at t=0, neglect the Coulomb interaction, and allow a single mode to couple at a single impurity site only.

## III. APPLICATION TO POLARON FORMATION

For the calculation we use energy units as eV, the time unit $\tau_0 = \dfrac{\hbar}{eV} \approx 0.65$fs, the unit of $\lambda_0$ is in $\mathrm{eV} \cdot \tau_0^{-1}$. We take $\varepsilon_l = 0$ $(l = 0, 1, 3, 4)$, $\varepsilon_2 = -0.2eV$, $\hbar\omega_0 = 0.1eV$. The impurity energy lowering is $\Delta E = |\varepsilon_2 - \varepsilon_0|$. We vary the parameters V, $\lambda_0$ and $\gamma_0$.

### A. Polaron formation and the band coupling

In all cases where there is bath coupling, the electron that starts at t=0 on a definite site and then obeys Eq. 15, invariably reaches a steady state population, irrespective of whether a localized polaron has formed or not. Switching the bath coupling on and off has a drastic effect of the time dynamics, as can be seen by comparing Fig. 2(a) and Fig. 2(b). As suggested by Zurek[7], the environment forces the quantum particle to behave classically, after a certain relaxation-decoherence time. Now consider the situation in which the particle actually localizes at the impurity site; we call this the polaron formation process. The reason for localization is a combination of two effects: i)the impurity site can have a lower energy and ii) it is coupled to a local vibration which is in turn coupled to a dissipative bath. Without the vibrations, the lower energy will not on its own cause localization.

It is useful to look at the localization dynamics in Fig. 2(b). In this figure the impurity population $P_2$ (in the stationary state) at long times is bigger than the population on other sites. Arrival or formation time of the polaron can be defined as the time point at which population $P_2$ reaches a certain value. In the same way as done in the experimental measurement by Lewis et al.[26] we define the "arrival time"as the time at which the target population reaches $\sim (1 - e^{-1} \approx 0.76)$ of its final

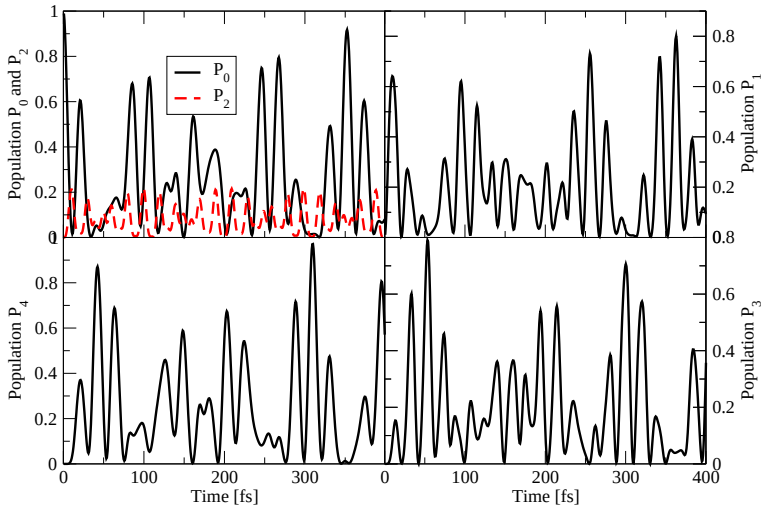


(a)

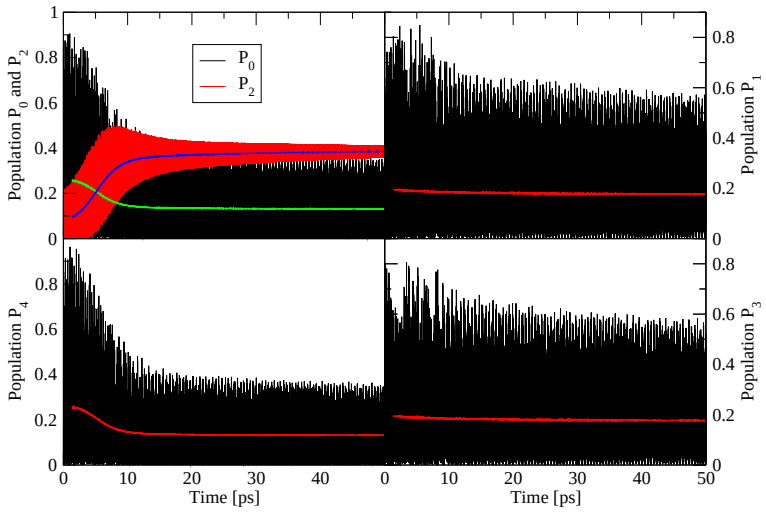


(b)

FIG. 2: Population distribution on different sites shown as a function of time. $\varepsilon_l = 0$ $(l = 0, 1, 3, 4)$, $\varepsilon_2 = -0.2eV$, $V = 0.1eV$, $\lambda_0\tau_0 = 0.01eV$, $\hbar\omega_0 = 0.1eV$, $\hbar\gamma_0 = 0.04eV$, $\tau_0 = \dfrac{\hbar}{eV} \approx 0.65$fs (femtosecond). In the left upper of panel (b), the green and blue lines indicate the average values of $P_0$ and $P_2$ respectively. In the other panels the red line indicates the average value of the oscillation shown in black. No electron-vibration coupling ($\alpha = 0$ in Eq. 2) was used for panel (a) and the dashed line indicates $P_2$.

value. Thus we use the criterion

$$\tilde{P}_2(\tau_p) = P_2^{\infty}(1 - e^{-1}) \ , \tag{21}$$

here $\tilde{P}_2(\tau_p)$ is the "time-averaged "value of $P_2$ at time $\tau_p$, obtained by averaging the points within the range $\tau_p \pm 50fs$ (femtoseconds). $P_2^{\infty}$ is the time-averaged value of $P_2$ in the long time limit ($P_2^{\infty}$ is plotted in the supporting information for varying $\lambda_0$, $\gamma_0$ and V). This $\tau_p$ is the arrival time, also defined as the population formation time[56].

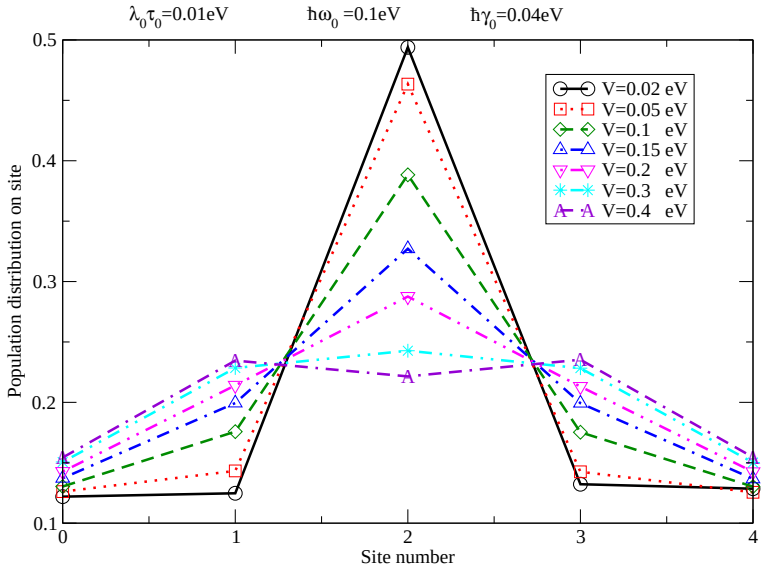


(a)

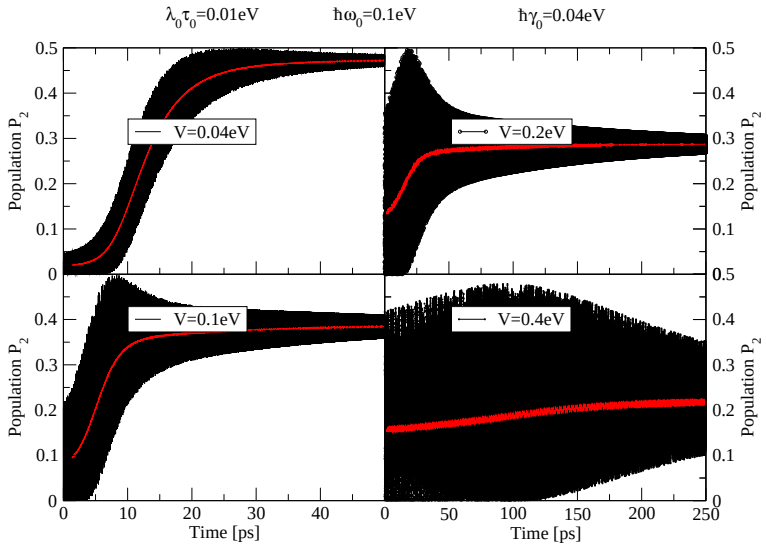


(b)

FIG. 3: (a): Stationary population distribution on different sites $l$ with different band coupling V. (b): Population ($P_2$) shown as a function of time. $\varepsilon_l = 0$ ($l = 0, 1, 3, 4$), $\varepsilon_2 = -0.2eV$, $\lambda_0\tau_0 = 0.01eV$, $\hbar\omega_0 = 0.1eV$, $\hbar\gamma_0 = 0.04eV$, $\tau_0 = \dfrac{\hbar}{eV} \approx$ 0.65fs(femtosecond). In panel (b) the red line indicates the average value of the oscillation shown in black.

We now ask a) when does a polaron form (for given values of the vibronic coupling, impurity energy and relaxation parameters), b)when does the electron localize at the impurity site for a given tunneling matrix element V? Fig. 3(a) plots the steady state population for different band couplings V with a fixed impurity energy lowering $\Delta E$. The population on site 2 decreases with increasing V, as the population tends to equalize on neighboring sites. This means that for V much larger than the averaged electron-vibration coupling energy $F(t)$, no polaron is formed, the population is delocalized and tends to be a number $\sim$ 1/N at each site (strictly 1/N applies only to periodic

boundary conditions). Note that for a symmetric chain with one site coupling in the middle only, the population at that one coupled site never exceeds 0.5[57]. This is an artifact of the simple model. When coupling is extended to other sites and/or symmetry is broken, the population can indeed reach 1. For a long chain, the local density tends to 0 as 1/N, and thus longer chains need stronger vibronic coupling to localize the particle. The combination of the local energy lowering $\Delta E$ and the electron-vibration coupling energy must be large enough to compensate for the localization energy cost.

In Fig. 3(b) $P_2(t)$ is plotted for different values of V, showing how strong the polaron localization is. For a small value of V=0.04eV, the localized population is larger than $\frac{1}{5}$ as one would expect, and the population (localized state ) formation time (in Eq. 21) is longer. At higher V, the localized population becomes smaller and the formation time shortens since carriers reach their destination more quickly (see Fig. 3(b) with V=0.1eV).

For a large V=0.4eV, the local population is fairly uniform and we can no longer talk of localization or polaron formation as shown in the bottom-right panel of Fig. 3(b). The population reaches steady state very slowly and its long time average value is of the order of $\frac{1}{5}$ (see Fig. S3 in the support information). The crossover occurs roughly when the half bandwidth 2V exceeds the localization energy.

Besides the bond coupling $V$, the different total site number $N$ influences the population distribution. As shown in Fig. 4, the middle site always has the largest population because that is where the polaron forms. The population on the other sites will decrease with increasing $N$. By assuming that the defect and the electron-vibration coupling always occur on the middle site, and that the starting condition is that the electron begins to transfer from site 0, after a certain access time the middle site will always have the largest population. The long time population on each of the other sites will decrease with increasing $N$.

### B. Electron-vibration coupling and vibration-phonon coupling relaxation rate

We now examine the influence of the electron-vibration coupling $\lambda_0$ and the vibration-phonon dissipation rate $\gamma_0$ on the population formation time; results are shown in Fig. 5(a). We see that the formation time decreases with increasing $\lambda_0$ but then saturates. The dissipation rate is crucial in localizing the particle. This rate also determines the strength of the oscillations as can be seen from Fig. 6. In large closed systems one can in some limits arrive at polaron formation[14]. But in a physical molecular environment, energy dissipation is necessary. Fig. 5(b) is a 3D plot of the formation time

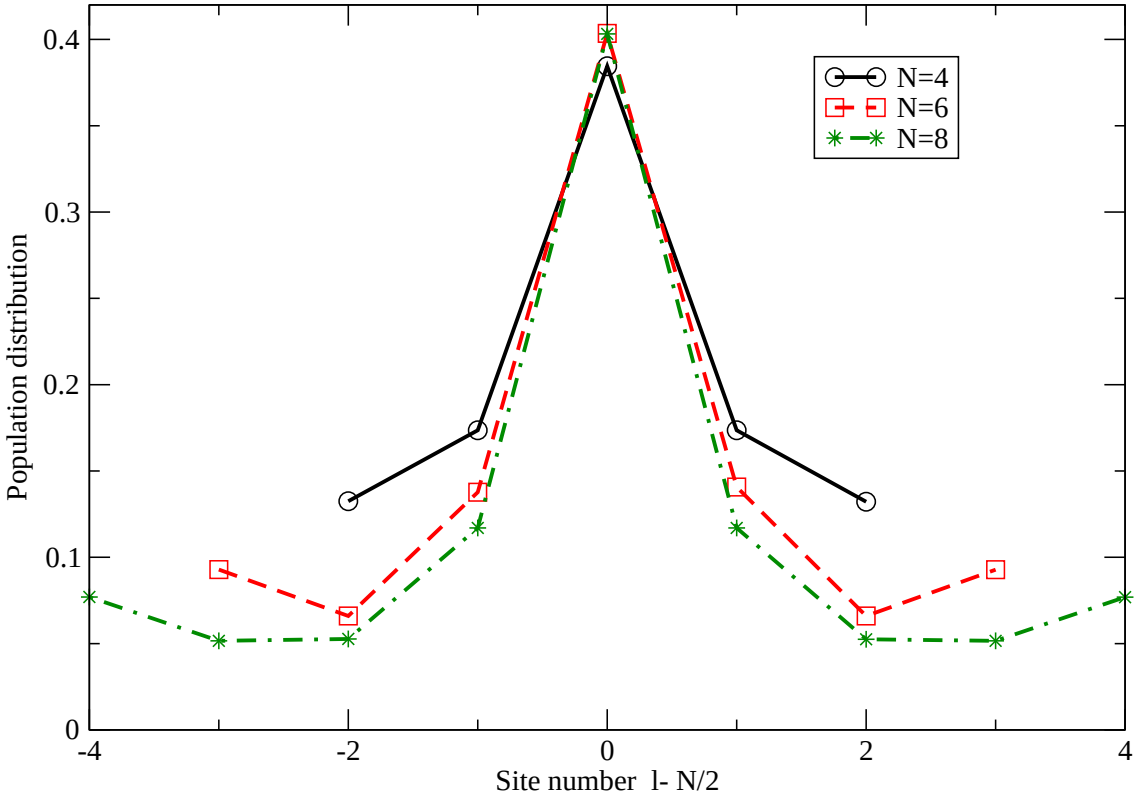


FIG. 4: Population distribution on site $l$ shown with different total site number $N$. In X-axis, 0 indicates the middle site ($N/2$ with $N$ being even number). $\varepsilon_l = 0$ but with the middle site energy $\varepsilon_{N/2} = -0.2eV$, V $= 0.1eV$, $\hbar\omega_0 = 0.1eV$, $\hbar\gamma_0 = 0.04eV$, $\tau_0 = \frac{\hbar}{eV} \approx 0.65$fs(femtosecond).

as a function of V and $\lambda_0$ (3D plots of the formation time as a function of V and $\gamma_0$ can be found in the supporting information). The apparent turnover with increasing V (Fig. 5(b)) in the population formation time beyond V$\sim$0.06eV for small electron-vibration coupling $\lambda_0$ occurs because for large V, the excitation relaxes into a population that is no longer strictly speaking a localized polaron. The population distribution is roughly constant in this limit as exhibited in Fig. 5(b). The "population formation time"should now be simply a population relaxation time (time to reach the steady state).

### C. Energy relaxation

Let us now apply these techniques to describe the experiments of the Wolf and Harris groups[33,43]. This last observation could be another crucial and interesting variable in materials/interfaces with low work functions and with large polaron energies. This type of experiment has been carried out with various organic overlayers[43]. An example of the energy relaxation scenario that matches the range of experimental parameters is shown in Fig. 7. The relaxation of energy is faster with increasing $\lambda_0$. Here ice is grown with different thicknesses on various metals. Charges are injected by

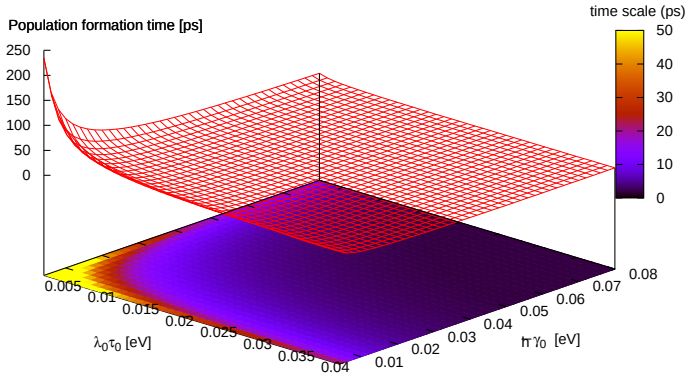


(a)

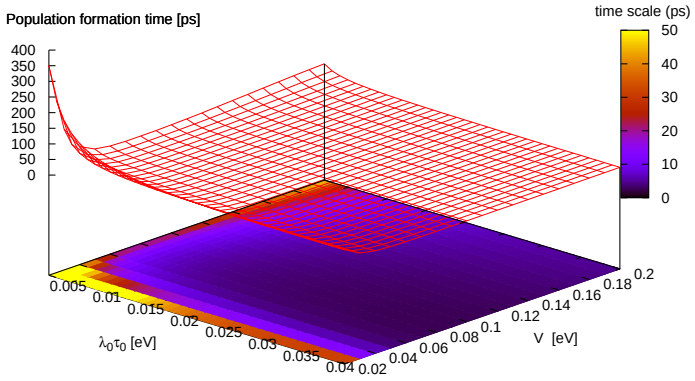


(b)

FIG. 5: (a): Population formation time $\tau_p$ (Eq. 21) shown as a function of the electron-vibration coupling parameter $\lambda_0$ and vibration-phonon coupling relaxation parameter $\gamma_0$. (b): Population formation time $\tau_p$ (Eq. 21) shown as a function of the nearest neighbor site coupling parameter V and $\lambda_0$. $\varepsilon_l = 0$ ($l = 0, 1, 3, 4$), $\varepsilon_2 = -0.2eV$, V $= 0.1eV$, $\hbar\omega_0 = 0.1eV$, $\hbar\gamma_0 = 0.04eV$, $\tau_0 = \dfrac{\hbar}{eV} \approx 0.65$fs(femtosecond).

femtosecond pulses from the metal electrode into the interfacial image potential band. From here the charges relax into the conduction band of the ice where they start digging in and building polarons. Depending on the thickness of the ice layer, and its amorphous or crystalline nature, the polaron will form on different time scales. The energy of the particle is monitored on a picosecond scale by an energy and angle resolved photoemission process. The thickness of the ice affects the coupling strength, the frequency of the phonon modes, and the relaxation rate of the water dipoles. The metastable charge will eventually relax back into the metal but it has to tunnel through a barrier.

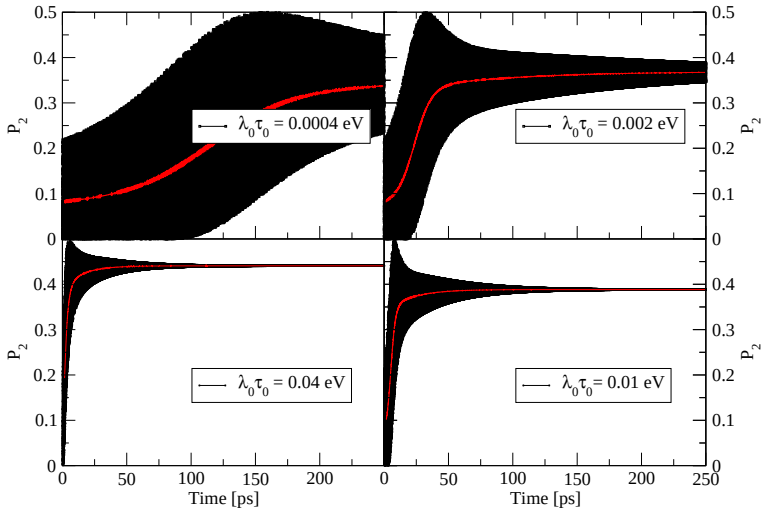


(a)

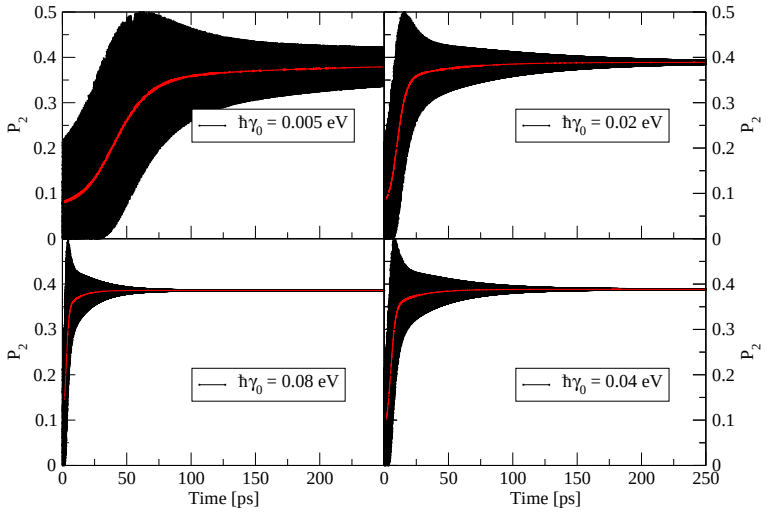


(b)

FIG. 6: (a)Population $P_2$ shown as a function of time with different electron-vibration coupling parameter $\lambda_0$ and the vibration-phonon coupling dissipation rate relaxation parameter $\gamma_0 = 0.04eV$. (b) Population $P_2$ shown as a function of time with different phonon bath relaxation parameter $\gamma_0$ and $\lambda_0\tau_0 = 0.01eV$. $\varepsilon_l = 0$ $(l = 0, 1, 3, 4)$, $\varepsilon_2 = -0.2eV$, V $= 0.1eV$, $\hbar\omega_0 = 0.1eV$, $\tau_0 = \dfrac{\hbar}{eV} \approx 0.65$fs(femtosecond). The red line indicates the average value of the oscillation shown in black.

The tunnel rate depends on the energy of the electron, and the returning charge can only tunnel to empty states inside the metal (above the fermi energy). No attempt is made to fit the data, but we give a proof of principle. For the electron solvation problem, the local energy lowering $\Delta E$ will be due to the electronic polarization of the medium, and the induced rotation of the water dipoles will produce terms very similar to the dynamic bath terms in our Hamiltonian. Here we use the limit $\gamma_0 \gg \omega_0$ and also a large $\lambda_0$ to simulate the vibronic coupling.

Fig. 7 illustrates the energy relaxation as a function of time. Wolf et al[33] have shown that the thinner the ice layer, the faster the electron loses its energy to the bath, deforming the medium.

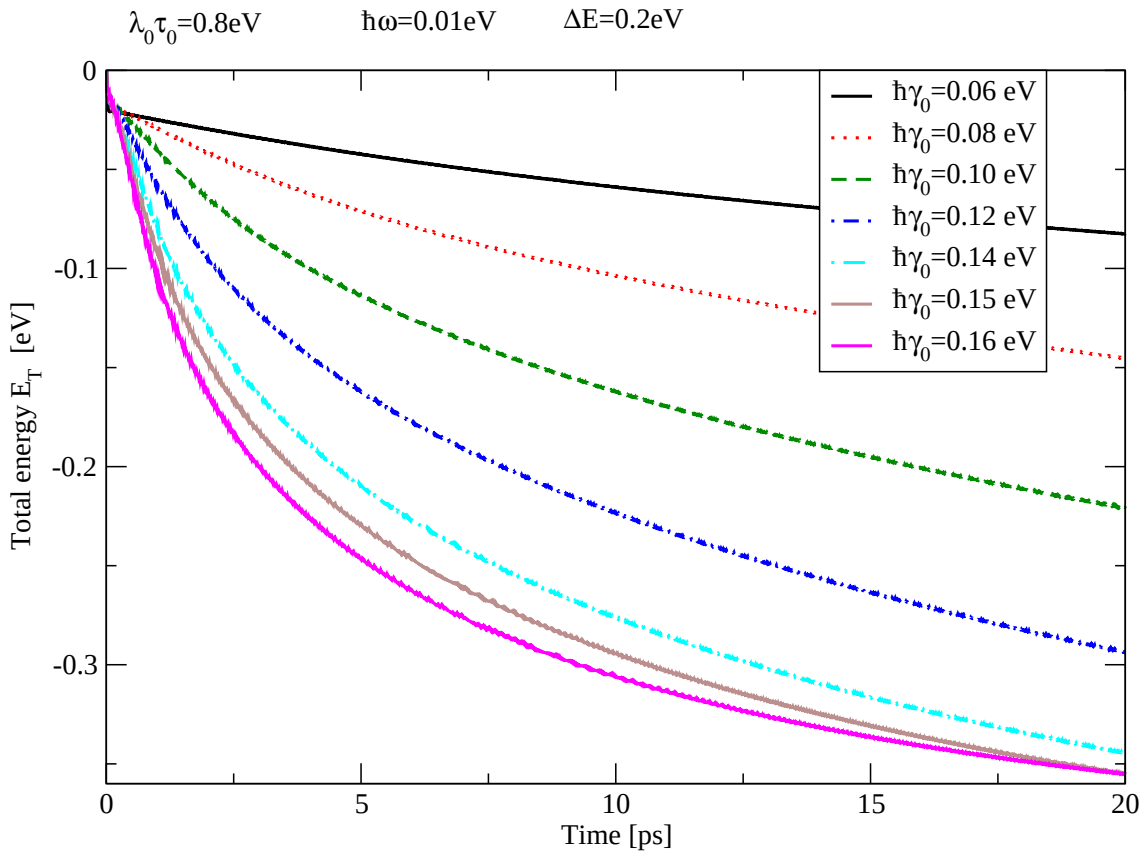


FIG. 7: Total system energy $E_T$ shown as a function of time with different vibration-phonon coupling dissipation rate $\gamma_0$ and $\Delta E = 0.2eV$. $\varepsilon_l = 0$ $(l = 0, 1, 3, 4)$, $\varepsilon_2 = -0.2eV$, V $= 0.1eV$, $\lambda_0\tau_0 = 0.8eV$, $\hbar\omega_0 = 0.01eV$, $\tau_0 = \frac{\hbar}{eV} \approx 0.65$fs(femtosecond).

Fig. 7 illustrates how this effect can be simulated within the present model, showing how the energy relaxation can be varied by varying the dissipation rate $\gamma_0$. The fast dissipation rate means rapid relaxation of the lattice coordinates to their final values. This implies that the energy reaches its optimal "polaronic" value in a shorter time. This agrees with the arguments given by Wolf et al[33]: Water dipoles in thin layers are more mobile than in thick layers. A realistic simulation would need a detailed consideration of the relevant modes and coupling strengths. Temperature can be built in by adding a noise term in Eq. 7 and carrying out the full stimulation of the displacement, not just the relaxation.

## IV. CONCLUSION

We have developed a methodology and demonstrated that by considering quantum motion with bath coupling, local energy differences, and energy dissipation, one can achieve dynamic localization of carriers. More generally we can understand how a particle which started on a quantum trajectory,

becomes dephased as a result of the bath interaction. This removes the quantum oscillations and one ends up with a well defined steady state population on each site. The ion displacements are treated by semi-classical Ehrenfest dynamics which may introduce errors. The method is applicable to electrons or excitons, and the bath modes can be any boson modes, provided the bath coordinates can in good approximation, be described in terms of semi-classical dynamics. Subject to the previous restrictions, we can determine (by simulation) how fast the localized polaron forms.

At long time, the quantum trajectory relaxes into a classical distribution[7]. The general sketch shown in Fig.1 gives an idea of the range of problems where the present method can be applied. The conclusion reached here agrees in spirit with those reached by Emin and Kriman[1,44,45] using the Holstein diatomic polaron lattice model. These authors showed that the polaron formation depends critically on the tunneling energy $V$ and the width of the phonon Bloch band, with the population formation time $\tau_p$ (Eq. 21) potentially varying from $10^{-13}$ to 1 second. The phonon bandwidth plays a similar role to the dissipation rate in our finite size model since once emitted into the extended lattice, the energy of the phonons will not return. But as pointed out right at the start, the semi-classical treatment of the bath has its problems. The vibrations do not see the "actual"but the expectation value of the charge density . Also, the zero point point motion of the lattice is neglected. In parameter ranges where phonon modes are well resolved, and splittings larger or comparable to electron bandwidths[19], the semi-classical approach will tend to overestimate the relaxation times but still work well to obtain steady state values.

Finally, we note that in the classical bath description, temperature can be introduced by allowing thermal modulation of the bath modes. Thus a localized polaron formed by the dynamical terms can be dislodged by the thermal force term[15] which has to be introduced in Eq. 15. The thermal fluctuations self-consistently modulate the local population and tend to prevent localization. They will cause hopping transport in our model. However it have been proposed that thermal fluctuations can cause localization in the linear system of degenerate states and in that case, the transport can not be described by hopping[46,47], for example, for the crystalline organic semiconductors at room temperature. Where the thermal molecular motions cause large fluctuations in the intermolecular transfer, which destroys the translational symmetry of the electronic Hamiltonian and in turn localize the charge carrier. Such a puzzling transport regime can be understood from the simultaneous presence of band carriers and incoherent states that are dynamically localized by the thermal lattice disorder. However it has been shown that thermal fluctuations can also (under certain circumstances) increase disorder and cause localization[46,47]. In these cases, one cannot say that the

transport proceeds simply by hopping. Motion takes place by way of a more subtle interplay of coherent and incoherent processes. Here thermal molecular motions cause large fluctuations in the intermolecular transfer, which destroys the translational symmetry of the electronic Hamiltonian and in turn localizes the charge carrier. It has been suggested[46,47] that the transport involves the simultaneous presence of band carriers and incoherent states, which can be dynamically localized and delocalized by thermal fluctuations. Particles which at temperature T=0 would normally want to form localized populations at selected localization sites will, at temperature $T \neq 0$, move both by coherent tunneling and by hopping transport using the thermal forces which act on diagonal and tunneling terms $V[|\tilde{R}_{ij}|]$[14,42]. However, given the limited vibrational space one can use in practice, and all the related unknowns, there is no guarantee that thermodynamic limits will be reached in systems with wide energy separations.

**Acknowledgement:** We thank Abraham Nitzan for his useful discussions and insightful comments. This work was supported by the Non-Equilibrium Energy Research Center (NERC) which is an Energy Frontier Research Center funded by the U.S. Department of Energy, Office of Science, Office of Basic Energy Sciences under Award Number DE-SC0000989. MR thanks the chemistry division of the NSF (CHE-1058896) for support. G. Li thanks Feifei Li for useful discussions.

---

[1] D. Emin, *Polarons* (University Press, Cambridge, 2012).

[2] J. Bonča and S. A. Trugman, Phys. Rev. Lett. **75**, 2566 (1995).

[3] S. Yeganeh, M. Galperin, and M. Ratner, J. Am. Chem. Soc. **129**, 13313 (2007).

[4] L. H. Yu, Z. K. Keane, J. W. Ciszek, L. Cheng, M. P. Stewart, J. M. Tour and D. Natelson, Phys. Rev. Lett. **93**, 266802 (2004).

[5] Z. An, C. Q. Wu, and X. Sun, Phys. Rev. Lett. **93**, 216407 (2004).

[6] Y. Zhao, B. Luo, Y.-Y. Zhang, and J. Ye, J. Chem. Phys. **137**, 084113 (2012).

[7] W. H. Zurek, Rev. Mod. Phys. **75**, 715 (2003).

[8] C. J. Brabec, G. Zerza, G. Cerullo, S. D. Silvestri, S. Luzzati, J. C Hummelen and S. Sariciftci, Chem. Phys. Lett. **340**, 232 (2001).

[9] G. S. Beddard, Phil. Trans. R. Soc. A **356**, 421 (1998).

[10] M. Galperin, M. A. Ratner, A. Nitzan, and A. Troisi, Science **319**, 1056 (2008).

[11] M. Saitoh, Journal of Physics C: Solid State Physics **5**, 914 (1972).

[12] B. Movaghar, Semicond. Sci. Technol. **2**, 185 (1987).

[13] P. W. Anderson, Phys. Rev. **109**, 1492 (1958).

[14] G. Kopidakis, C. M. Soukoulis, and E. N. Economou, Phys. Rev. B **51**, 15038 (1995).

[15] M. Galperin, M. A. Ratner, and A. Nitzan, Nano Letter **5**, 125 (2005).

[16] V. D. Lakhno, Phys. Chem. Chem. Phys. **4**, 2246 (2002).

[17] V. D. Lakhno, J. Bio. Phys. **31**, 145 (2005).

[18] V. D. Lakhno and A. Korshunova, Mathematical Biology & Bioinformatics. **5**, 1 (2010).

[19] G.-Q. Li, B. Movaghar, A. Nitzan, and M. A. Ratner, J. Chem. Phys. **138**, 044112 (2013).

[20] K. Kneipp, M. Moskovits, and H. Kneipp, In Topics in Applied Physics; Springer: Berlin and Heidelberg **103**, 221 (2006).

[21] G. Grancini, D. Polli, D. Fazzi, J. Cabanillas-Gonzalez, G. Cerullo and G. Lanzani, J. Phys. Chem. Lett. **2**, 1099 (2011).

[22] P. N. Ciesielski, D. E. Cliffel, and G. K. Jennings, J. Phys. Chem. A **115**, 3326 (2011).

[23] E. A. Weiss, G. Katz, R. H. Goldsmith, M. R. Wasielewski, M. A. Ratner, R. Kosloff and A. Nitzan, J. Chem. Phys. **124**, 074501 (2006).

[24] R. D. Pensack and J. B. Asbury, J. Phys. Chem. Lett. **1**, 2255 (2010).

[25] F. C. Grozema, S. Tonzani, Y. A. Berlin, G. C. Schatz, L. D. A. Siebbeles and M. A. Ratner, J. Am. Chem. Soc. **130**, 5157 (2008).

[26] F. D. Lewis, H.-h. Zhu, P. Daublain, T. Fiebig, M. Raytchev, Q. Wang and V. Shafirovich, J. Am. Chem. Soc. **128**, 791 (2006).

[27] A. Nitzan and M. A. Ratner, Science **300**, 1384 (2003).

[28] A. Nitzan, *Chemical Dynamics in condensed Phases* (Oxford, Oxford, 2006).

[29] A. Aviram and M. A. Ratner, Chem. Phys. Lett. **29**, 277 (1974).

[30] P. Xiong, J. M. Nocek, J. Vura-Weis, J. V. Lockard, M. R. Wasielewski and B. M. Hoffman, Science **330**, 1075 (2010).

[31] T. Brixner, J. Stenger, H. M. Vaswani, M.-H. Cho, R. E. Blankenship and G. R. Fleming, Nature **434**, 625 (2005).

[32] C. Rischel, D. Spiedel, J. P. Ridge, M. R. Jones, J. Breton, J.-C. Lambry, J.-L. Martin and M. H. Vos Proc. Natl. Acad. Sci. USA **95**, 12306 (1998).

[33] C. Gahl, U. Bovensiepen, C. Frischkorn, and M. Wolf, Phys. Rev. Lett. **89**, 107402 (2002).

[34] G. D. Filippis, V. Cataudella, A. S. Mishchenko, C. A. Perroni and J. T. Devreese, Phys. Rev. Lett. **96**, 136405 (2006).

[35] S. Meshkov, Sov. Phys. JETP **89**, 1734 (1985).

[36] K. Huang and A. Rhys, Proc. R. Soc. Ser. A **204**, 406 (1950).

[37] Y. E. Perlin, Sov. Phys. Uspekhi **6**, 542 (1964).

[38] Y. E. Perlin, B. S. Tsukerblat, and E. Perepelitsa, Sov. Phys. JETP **62**, 2265 (1972).

[39] S. Henrik, *Introduction to Quantum Mechanics* (World Scientific Pub Co Inc., New Jersey, 1991), pp. 108–109.

[40] G. Katz, D. Gelman, M. A. Ratner, and R. Kosloff, J. Chem. Phys. **129**, 034108 (2008).

[41] N. Renaud, M. A. Ratner, and V. Mujica, J. Chem. Phys. **135**, 075102 (2011).

[42] A. J. Heeger, S. Kivelson, J. R. Schreiffer, and W. P. Su, Rev. Mod. Phys. **60**, 781 (1988).

[43] P. Szymanski, S. Garrett-Roe, and C. B. Harris, Progress in Surface Science **78**, 1 (2005).

[44] D. Emin and A. M. Kriman, Phys. Rev. B **34**, 72787289 (1986).

[45] D. Emin, Monatsh Chem **144**, 3 (2012).

[46] S. Fratini and S. Ciuchi, Phys. Rev. Lett. **103**, 266601 (2009).

[47] A. Troisi and G. Orlandi, Phys. Rev. Lett. **96**, 086601 (2006).

[48] G.-Q. Li, B. Movaghar, and M. A. Ratner, Electron-phonon interaction induced electron localization on a 2D layer, to be submitted.

[49] D. Emin, Advances in Physics **22**, 57 (1973).

[50] Y. A. Firsov, *Polarons* (Nauka, Moscow, 1975).

[51] G. L. Sewell, *Polarons and Excitons* (Plenum Press, New York, 1963).

[52] T. Holstein, Ann. Phys. **8**, 325 (1959).

[53] M. I. Klinger, *Problems of Polaron Transport Theory* (Pergamon Press, Oxford, 1979).

[54] The model has been extended to larger systems and to two-dimensions. The conclusions reached are essentially the same[48].

[55] The problem of an electron moving in a tight-binding lattice in the presence of electron-vibration coupling is not new, and

there exists a vast literature on this subject[49–53]. But this previous work is almost always concerned with equilibrium states. In the present analysis the emphasis is on the non-equilibrium dynamics, and the primary motive is not only to study polaron formation, but also to demonstrate how the electron-vibration coupling in non-periodic and nanoscale systems gives rise to dephasing, and in some cases localization and polaron formation.

[56] In the finite system considered, with dissipation, and with given initial conditions for time t=0, the particle will eventually reach a steady state distribution, whatever parameters we chose. This population relaxation time has a characteristic time scale which we must define. We adopt the experimental definition that it is the time at which the population has reached $(1 - e^{-1})$ of its "final value". In some cases, with appropriate parameters, tunneling term, electron-phonon coupling and diagonal energies, the final population can evolve to become a state localized in a region of space, in which case we speak of a polaron having formed. The polaron formation time scale is defined in the same way.

[57] see Figs. S4-S6 in the support information and Fig.4 in reference 16.